Rapid Communications

Analog of electromagnetically induced transparency based on magnetic plasmonic artificial molecules with symmetric and antisymmetric states

Zhixia Xu,* Siyuan Liu, Shunli Li, and Xiaoxing Yin†
State Key Laboratory of Millimeter Waves, Southeast University, Nanjing 210096, China

(Received 29 October 2018; published 4 January 2019)

We report a classical electromagnetically induced transparency (EIT) analog based on magnetic plasmonic artificial molecules consisting of magnetic localized surface plasmons and split ring resonators. The key to achieve EIT-like transparency are the excited symmetric and antisymmetric states based on bright-dark mode coupling, where the bright mode of the split ring resonator excited by incident waves is coupled to the dark mode of the neighbor spoof magnetic localized surface plasmons resonator. We conduct experiments, simulations, and analysis based on the Lorentz oscillator model. In addition, we numerically demonstrate that the EIT-like transparency can be employed to permittivity sensing applications.

DOI: 10.1103/PhysRevB.99.041104

Electromagnetically induced transparency (EIT) is a destructive interference that causes a sharp transmission window within the absorption band in a coherently driven atomic system [1,2]. The high-Q transparency peak, as well as the drastic change of dispersion, has many practical applications, such as quantum memory [3,4], nonlinearity enhancement [5], and sensors [6]. Recently, researchers have found that the EIT-like phenomena can occur in many classical coupled Lorentz oscillator systems, such as coupled microcavities [7], waveguide resonators [8], and optomechanical systems [9]. Particularly, artificial materials, named as metamaterials (MMs), can be configured to obtain EIT-like spectra ranging from optical band to acoustic band [10–17]. Mode coupling is the key to obtain EIT analog in MMs. A bright mode, usually a low-Q-factor mode, is a mode which can be excited by incident wave directly. In contrast, the dark mode, usually a high-Q-factor mode, cannot be excited by incident wave directly, it can be near-field coupled to the bright mode. Two approaches can be utilized to generate an EIT analog: bright-dark mode coupling [12,13,17–21] and bright-bright mode coupling [22–24]. At least one bright mode is necessary to couple energy from external incident waves. Then, other resonators, whether bright or dark, are involved to establish a coupled Lorentz oscillator model, which is the core of an EIT analog in MMs. Among these EIT-analog systems, plasmonic structures are widely utilized because of the strong response of metal at the optical band [25–27]. However, it seemed difficult to realize surface-plasmonlike behavior on metal at a low-frequency band for a long time, until the proposal of spoof surface plasmons (SSPs), which extend the study of surface plasmons to terahertz and microwave band [28–31]. Recently, a simple SSP structure was successfully proposed to realize an EIT analog [32]. The interesting structure consists of prism-coupled double-layer arrays with symmetric and antisymmetric resonances, leading to a transparency window.

Inspired by the pioneering work [32], we report an EIT analog based on bright-dark mode coupling between split ring resonators (SRRs) and spoof magnetic localized surface plasmons (S-MLSPs). Note that S-MLSPs were recently proposed [33] as a counterpart to spoof electric localized surface plasmons [34], making it possible to investigate magnetic plasmonic excitations. In this paper, artificial "molecules" consist of SRRs and S-MLSPs, which can be regarded as bright "atom" and dark "atom," respectively. Only the SRR, the bright atom, can be excited by the external field, and it interacts with neighbor S-MLSPs, the dark atom, via near-field coupling. In/out-of-phase retardations are involved to establish symmetric and antisymmetric states of the molecules. Between the two states exists the EIT-like sharp transparency. We treat the structure as a coupled Lorentz oscillator model, and theory, simulations, and experiments match well. Moreover, we numerically demonstrate the potential sensing applications of the presented EIT analog for permittivity of the surrounding environment.

Figure 1 shows the proposed structure schematically. In the topology, a 35-um-thick metallic layer is etched on the top layer of the 0.6-mm-thick FR-4 dielectric substrate. Each unit, artificial molecule, consists of paired SRR and S-MLSP. Only SRR, the bright atom, is excited by a normally incident plane wave with y-axis polarized electric field and x-axis polarized magnetic field. Figure 2 shows the formation of the proposed EIT-analog system. Due to the external electric field parallel to the split, SRR can be excited to a magnetic-dipole resonance where circular current flow exists on the SRR without any contribution to an electric-dipole moment [35], which makes SRR an ideal magnetic bright atom. From Ref. [33], it is known that a spiral-like resonator can support both electric- and magnetic-dipole modes, and the resonant frequencies depend on the geometric parameters of the resonator. In the proposed schematic, the incident waves cannot excite the magnetic resonance, and near-field coupling is the only way to excite S-MLSP whose magnetic resonant frequency is designed the same as the magnetic-resonant frequency of SRR, making S-MLSP an ideal magnetic dark

*230159363@seu.edu.cn
†101010074@seu.edu.cn

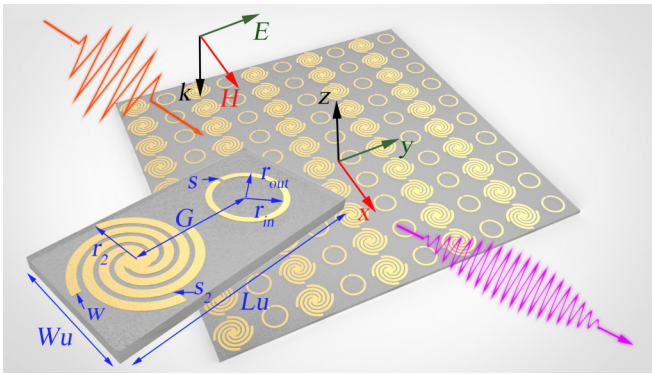

FIG. 1. Schematic of the proposed EIT analog based on magnetic plasmonic structures, where the detailed view of a single molecule is also presented. 0.035-mm-thick copper is etched on the top layer of 0.6-mm-thick FR-4 substrate. The distance of the center of paired magnetic atom is G. Outside radius, inside radius, and split width of SRR are represented as r_{out}, r_{in}, and s, respectively. Radius, the width of the four wrapped copper arms, and the gap width of the S-MLSP are represented as r_2, w, and s_2. The geometric dimensions of the presented model are $r_{\text{out}} = 1.9\,\text{mm}$, $r_{in} = 1.6\,\text{mm}$, $s = 0.2\,\text{mm}$, $r_2 = 2.9\,\text{mm}$, $w = 0.4\,\text{mm}$, and $s_2 = 0.2\,\text{mm}$

atom. Similar to what happens in planar SRR arrays [36–38], magnetoinductive waves play tricks behind the excitation of S-MLSP. When SRR is excited by external waves, its energy is transferred to the S-MLSP by magnetoinductive waves. The transverse coupling between the pair of atoms gives birth to antisymmetric and symmetric states, which can be regarded as an analog of atoms at two reversed orbitals. Two atoms oscillate out/in-phase whose magnetic moments are hybridized antiparallel and parallel, respectively.

To vindicate the proposed EIT-analog system, we conduct simulations, experiments, and theoretical analysis. The fabricated sample and experimental environment are shown in Fig. 3(a). The sample, shown in Fig. 3(b), is fabricated in the anechoic chamber. A pair of tapered slot antennas for shot-pulse applications working from 3 to 20 GHz [39] is placed on both sides of the sample and linked to a vector network analyzer (Keysight PNA N5224A) by phase-compensated cables. Transmission and group delay curves are shown in Figs. 3(c) and 3(d), where we select both sides of the sample as two reference planes [40]. Experimental and numerical results obtained from COMSOL MULTIPHYSICS match well, and it is evident to observe the sharp EIT-like transparency along with the slow-light characteristic. Two resonant stop bands appear in the spectra, centered on 8.6 GHz ($\omega_-/2\pi$) and 9.15 GHz ($\omega_+/2\pi$), respectively, which correspond to antisymmetric and symmetric states of the artificial magnetic molecule discussed above. Distributions of magnetic and electric along the z axis are shown in Fig. 2.

Then, we analyze the structure in detail. The energy-level scheme of the model is shown in Fig. 4. Similar to the recent process-coupled systems [12,17,19,22,41,42], the theoretical analysis of the proposed EIT-analog system is based on the coupled Lorentz oscillator model of bright and dark atoms with the same resonant frequency ω_0 under harmonic excitation $E_{in}(t) = E_{in}(\omega)e^{-i\omega t}$

$$\frac{\partial^2 S_b(t)}{\partial t^2} + \gamma_b \frac{\partial S_b(t)}{\partial t} + {\omega_0}^2 S_b(t) = \frac{q_b}{m_b} E_{in}(t) - \kappa^2 S_d(t), \tag{1}$$

$$\frac{\partial^2 S_d(t)}{\partial t^2} + \gamma_d \frac{\partial S_d(t)}{\partial t} + {\omega_0}^2 S_d(t) = -\kappa^2 S_b(t). \tag{2}$$

$S_i, \gamma_i, q_i, m_i, \kappa (i = b \text{ or } d)$ are the effective displacement, loss factor, effective charge, effective mass, and coupling strength of the bright (b) and dark (d) atoms. The effective polarization χ_{eff} is obtained where C is the coefficient determined by effective charge and effective mass.

$$\chi_{\text{eff}} = \frac{q_b S_b + q_d S_d}{\varepsilon_0 E_{in}}, \tag{3}$$

$$\chi_{\text{eff}} = C \frac{\omega^2 - {\omega_0}^2 + i\omega\gamma_d}{\kappa^4 - \left(\omega^2 - {\omega_0}^2 + i\omega\gamma_d\right)\left(\omega^2 - {\omega_0}^2 + i\omega\gamma_b\right)}. \tag{4}$$

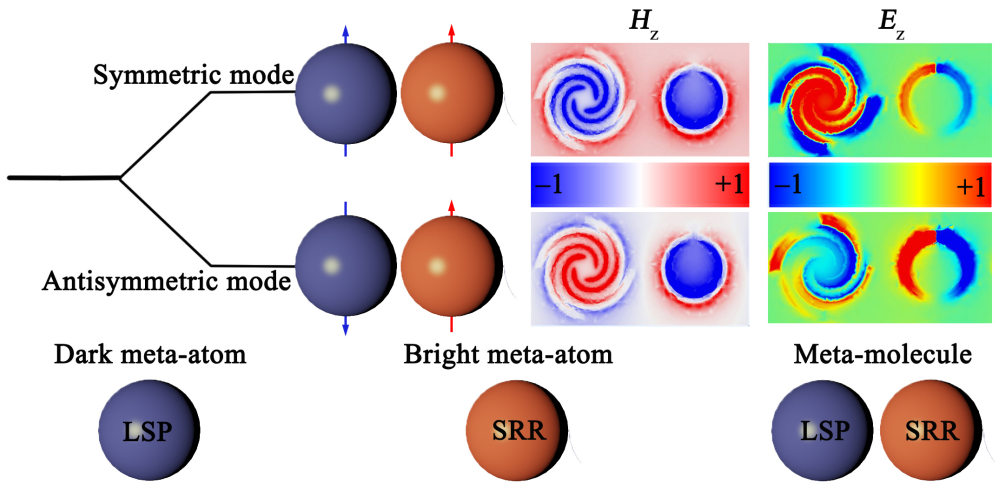

FIG. 2. Scheme of the artificial magnetic plasmonic molecule with antisymmetric and symmetric states. Inset picture shows corresponding magnetic and electric field along z axis.

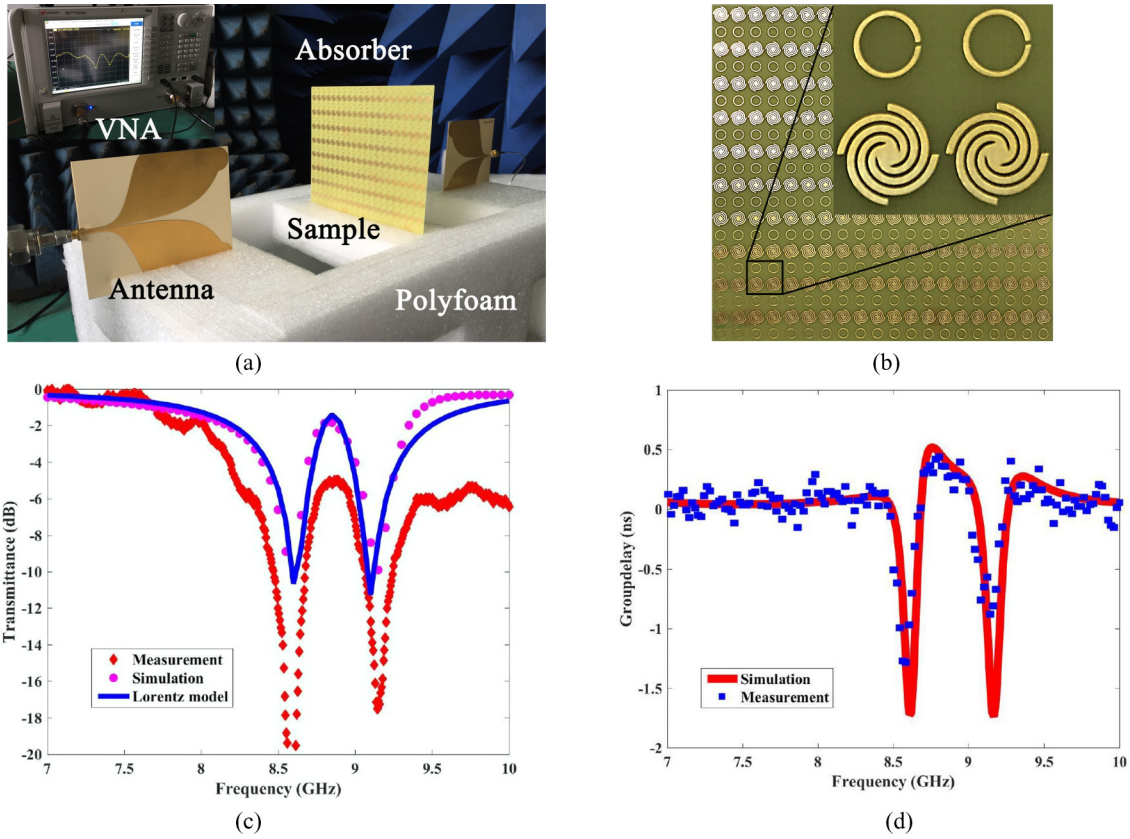

FIG. 3. (a) Experimental setup of the fabrication sample. (b) Photograph of the sample. (c) Numerical, experimental, and theoretical transmission curves. (d) Numerical and experimental group delay curves.

The transmission can be presented as

$$T = \left| \frac{4\sqrt{\chi_{\text{eff}}+1}}{(\sqrt{\chi_{\text{eff}}+1}+1)^2 e^{j(2\pi d/\lambda)\sqrt{\chi_{\text{eff}}+1}} - (\sqrt{\chi_{\text{eff}}+1}-1)^2 e^{-j(2\pi d/\lambda)\sqrt{\chi_{\text{eff}}+1}}} \right|. \tag{5}$$

In the proposed model, the transparency frequency ω_0 is 5.56×10^{10} rad/s (around 8.85 GHz), d is the thickness of the substrate (0.6 mm), and then we can estimate κ around 1.3×10^{10} rad/s using relationships among resonant transparency frequency and frequencies of antisymmetric and symmetric states mentioned before ($\omega_0{}^2 - \omega_-{}^2 = \kappa^2$ and $\omega_+{}^2 - \omega_0{}^2 = \kappa^2$).

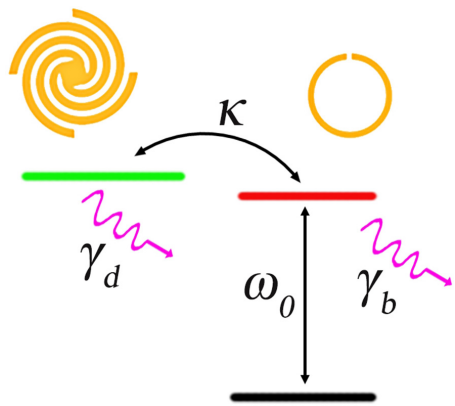

FIG. 4. Level scheme according to Lorentz oscillator model.

When we consider a lossless model, the width of the transparency window Ω can be written as

$$\Omega = \frac{\kappa^2}{\omega_0}. \tag{6}$$

We fit the numerical transmission curve in Fig. 3(c) where two sides of the metasurface are chosen as two reference ports. As pioneering researchers did recently [12,17,22], we obtain parameters for the proposed model by fitting the simulated results. Note that we have obtained thickness of the substrate d, coupling strength κ, and the transparency frequency ω_0. The remaining three unsolved parameters are coefficient C and loss factors γ_b and γ_d. Next, substituting the simulated transmission value for the proposed model at ω_0, ω_+, and ω_- into Eq. (5) leads to three equations listed below,

$$\begin{aligned} T(\omega_-) &= 0.101 \\ T(\omega_0) &= 0.655 \\ T(\omega_+) &= 0.102. \end{aligned} \tag{7}$$

Finally, combining and solving Eqs. (4)–(7), we can obtain the last three fitting parameters as follows: $C = 8.2 \times 10^{21}$,

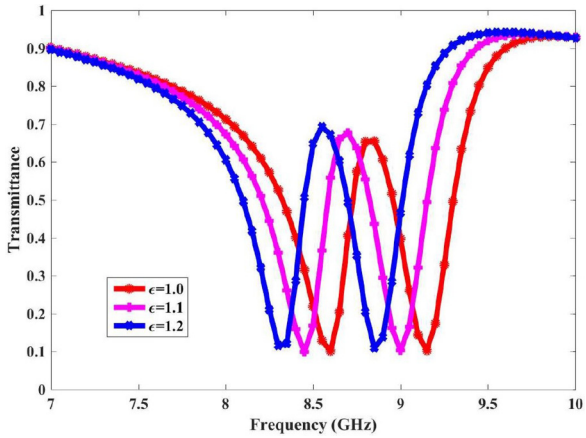

FIG. 5. Numerical transparency shift of the EIT-analog structure with respect to changes of the permittivity of the surrounding environment.

$\gamma_b = 3.15 \times 10^8$ rad/s, $\gamma_d = 4.35 \times 10^8$ rad/s. The experimental, simulated, and theoretical results match well in Fig. 3(c).

Due to the sharp EIT-like spectra and the ability of confined electromagnetic field, the proposed structure can be employed as a permittivity sensor at free space. It is foreseeable that the transparency frequency depends on the dielectric properties of the surrounding environment. The sensing ability of the proposed EIT-analog structure is demonstrated in Fig. 5. A clear shift of the transparency peak can be observed when increasing the permittivity ε of the surrounding environment from 1.0 to 1.2. The sensitivity can be defined as the shift of resonant peak per unit change of refractive index [43], amounting to about 12 mm/RIU.

In conclusion, we designed, fabricated, and analyzed a type of EIT analog working at microwave band, which consists of paired magnetic plasmonic resonators. We demonstrated that bright-dark mode coupling enables the formation of antisymmetric and symmetric states of the artificial molecule. The reported utilization of S-MLSP provides deep insights into the study of magnetic surface plasmons. The sharp transparency window and the large group delay of the EIT analog are useful for various practical applications, including slow-wave delay structures and sensors. As an example, we numerically present a permittivity sensing application based on the structure. Future work includes investigating bright-dark mode coupling in three-dimensional topology and designing stacked EIT-analog systems of magnetic plasmonic atoms.

This work was supported by National Natural Science Foundation of China (Grants No. 61427801, No. 61771127, No. U1536123, and No. U1536124), Scientific Research Foundation of Graduate School of Southeast University (Grant No. YBJJ1814), and Postgraduate Research & Practice Innovation Program of Jiangsu Province (Grant No. KYCX18_0098).

[1] K.-J. Boller, A. Imamoğlu, and S. E. Harris, Phys. Rev. Lett. **66**, 2593 (1991).
[2] S. E. Harris, Phys. Today **50**(7), 36 (1997).
[3] A. I. Lvovsky, B. C. Sanders, and W. Tittel, Nat. Photonics **3**, 706 (2009).
[4] K. M. Birnbaum, A. Boca, R. Miller, A. D. Boozer, T. E. Northup, and H. J. Kimble, Nature (London) **436**, 87 (2005).
[5] H. Tanji-Suzuki, W. Chen, R. Landig, J. Simon, and V. Vuletić, Science **333**, 1266 (2011).
[6] X. Zhou, L. Zhang, W. Pang, H. Zhang, Q. Yang, and D. Zhang, New J. Phys. **15**, 103033 (2013).
[7] B. Peng, S. K. Ozdemir, W. Chen, F. Nori, and L. Yang, Nat. Commun. **5**, 5082 (2014).
[8] R. D. Kekatpure, E. S. Barnard, W. Cai, and M. L. Brongersma, Phys. Rev. Lett. **104**, 243902 (2010).
[9] S. Weis, R. Rivière, S. Deléglise, E. Gavartin, O. Arcizet, A. Schliesser, and T. J. Kippenberg, Science **330**, 1520 (2010).
[10] A. A. Abdumalikov, Jr., O. Astafiev, A. M. Zagoskin, Y. A. Pashkin, Y. Nakamura, and J. S. Tsai, Phys. Rev. Lett. **104**, 193601 (2010).
[11] N. Papasimakis, V. A. Fedotov, N. I. Zheludev, and S. L. Prosvirnin, Phys. Rev. Lett. **101**, 253903 (2008).
[12] N. Liu, L. Langguth, T. Weiss, J. Kastel, M. Fleischhauer, T. Pfau, and H. Giessen, Nat. Mater. **8**, 758 (2009).
[13] N. Liu, S. Kaiser, and H. Giessen, Adv. Mater. **20**, 4521 (2008).
[14] H.-m. Li, S.-b. Liu, S.-y. Liu, S.-y. Wang, G.-w. Ding, H. Yang, Z.-y. Yu, and H.-f. Zhang, Appl. Phys. Lett. **106**, 083511 (2015).
[15] Y. Jin, Y. Pennec, and B. Djafari-Rouhani, J. Phys. D: Appl. Phys. **51**, 494004 (2018).
[16] R. Yahiaoui, M. Manjappa, Y. K. Srivastava, and R. Singh, Appl. Phys. Lett. **111**, 021101 (2017).
[17] F.-Y. Meng, Q. Wu, D. Erni, K. Wu, and J.-C. Lee, IEEE Trans. Microwave Theory Tech. **60**, 3013 (2012).
[18] J. Chen, P. Wang, C. Chen, Y. Lu, H. Ming, and Q. Zhan, Opt. Express **19**, 5970 (2011).
[19] P. Tassin, L. Zhang, R. Zhao, A. Jain, T. Koschny, and C. M. Soukoulis, Phys. Rev. Lett. **109**, 187401 (2012).
[20] J. Gu *et al.*, Nat. Commun. **3**, 1151 (2012).
[21] S. Xiao, T. Wang, T. Liu, X. Yan, Z. Li, and C. Xu, Carbon **126**, 271 (2018).
[22] R. Yahiaoui, J. A. Burrow, S. M. Mekonen, A. Sarangan, J. Mathews, I. Agha, and T. A. Searles, Phys. Rev. B **97**, 155403 (2018).
[23] M. Parvinnezhad Hokmabadi, E. Philip, E. Rivera, P. Kung, and S. M. Kim, Sci. Rep. **5**, 15735 (2015).
[24] K. M. Devi, D. R. Chowdhury, G. Kumar, and A. K. Sarma, J. Appl. Phys. **124**, 063106 (2018).
[25] V. Yannopapas, E. Paspalakis, and N. V. Vitanov, Phys. Rev. B **80**, 035104 (2009).
[26] T. Zentgraf, S. Zhang, R. F. Oulton, and X. Zhang, Phys. Rev. B **80**, 195415 (2009).

[27] G. Rana, P. Deshmukh, S. Palkhivala, A. Gupta, S. P. Duttagupta, S. S. Prabhu, V. G. Achanta, and G. S. Agarwal, Phys. Rev. Appl. **9**, 064015 (2018).
[28] J. B. Pendry, L. Martín-Moreno, and F. J. Garcia-Vidal, Science **305**, 847 (2004).
[29] J. N. Gollub, D. R. Smith, D. C. Vier, T. Perram, and J. J. Mock, Phys. Rev. B **71**, 195402 (2005).
[30] A. P. Hibbins, B. R. Evans, and J. R. Sambles, Science **308**, 670 (2005).
[31] Y. Nakata, T. Okada, T. Nakanishi, and M. Kitano, Phys. Rev. B **85**, 205128 (2012).
[32] K. Ooi, T. Okada, and K. Tanaka, Phys. Rev. B **84**, 115405 (2011).
[33] P. A. Huidobro, X. Shen, J. Cuerda, E. Moreno, L. Martin-Moreno, F. J. Garcia-Vidal, T. J. Cui, and J. B. Pendry, Phys. Rev. X **4**, 021003 (2014).
[34] A. Pors, E. Moreno, L. Martin-Moreno, J. B. Pendry, and F. J. Garcia-Vidal, Phys. Rev. Lett. **108**, 223905 (2012).
[35] N. Katsarakis, T. Koschny, M. Kafesaki, E. N. Economou, and C. M. Soukoulis, Appl. Phys. Lett. **84**, 2943 (2004).
[36] Z. Xu, S. Liu, S. Li, H. Zhao, L. Liu, and X. Yin, Appl. Phys. Express **11**, 042002 (2018).
[37] K. Hadjicosti, O. Sydoruk, S. A. Maier, and E. Shamonina, J. Appl. Phys. **117**, 163910 (2015).
[38] E. Shamonina, V. A. Kalinin, K. H. Ringhofer, and L. Solymar, J. Appl. Phys. **92**, 6252 (2002).
[39] S. Li, X. Yin, H. Zhao, and H. Qi, IEEE Trans. Antennas Propag. **63**, 3400 (2015).
[40] D. K. Ghodgaonkar, V. V. Varadan, and V. K. Varadan, IEEE Trans. Instrum. Meas. **38**, 789 (1989).
[41] Z. Xu, X. Cui, S. Liu, and X. Yin, Appl. Phys. Express **11**, 114002 (2018).
[42] F. Bagci and B. Akaoglu, J. Appl. Phys. **123**, 173101 (2018).
[43] C.-Y. Chen, I.-W. Un, N.-H. Tai, and T.-J. Yen, Opt. Express **17**, 15372 (2009).